Temporal increase in organic mercury in an endangered pelagic seabird assessed by century-old museum specimens

Anh-Thu E. Vo[a,b], Michael S. Bank[c], James P. Shine[c], and Scott V. Edwards[a,1]

[a]Department of Organismic and Evolutionary Biology, Museum of Comparative Zoology, Harvard University, Cambridge, MA 02138; [b]Museum of Vertebrate Zoology and Department of Integrative Biology, University of California, Berkeley, CA 94720; and [c]Department of Environmental Health, Harvard School of Public Health, Boston, MA 02215

Edited by Jerome Nriagu, University of Michigan, Ann Arbor, MI, and accepted by the Editorial Board March 23, 2011 (received for review September 19, 2010)

Methylmercury cycling in the Pacific Ocean has garnered significant attention in recent years, especially with regard to rising mercury emissions from Asia. Uncertainty exists concerning whether increases in anthropogenic emissions over time may have caused increased mercury bioaccumulation in the biota. To address this, we measured total mercury and, for a subset of samples, methylmercury (the bioaccumulated form of mercury) in museum feathers from an endangered seabird, the black-footed albatross (*Phoebastria nigripes*), spanning a 120-y period. We analyzed stable isotopes of nitrogen ($\delta^{15}N$) and carbon ($\delta^{13}C$) to control for temporal changes in trophic structure and diet. In post-1940 and -1990 feathers, we detected significantly higher mean methylmercury concentrations and higher proportions of samples exhibiting above deleterious threshold levels (~40,000 ng·g^{-1}) of methylmercury relative to prior time points, suggesting that mercury toxicity may undermine reproductive effort in the species. We also found higher levels of (presumably curator-mediated) inorganic mercury in older specimens of albatross as well as two nonpelagic species lacking historical exposure to bioavailable mercury, patterns suggesting that studies on bioaccumulation should measure methylmercury rather than total mercury when using museum collections. $\delta^{15}N$ contributed substantially to models explaining the observed methylmercury variation. After simultaneously controlling for significant trends in $\delta^{13}C$ over time and $\delta^{15}N$ with methylmercury exposure, year remained a significant independent covariate with feather methylmercury levels among the albatrosses. These data show that remote seabird colonies in the Pacific basin exhibit temporal changes in methylmercury levels consistent with historical global and recent regional increases in anthropogenic emissions.

Asian emissions | ecotoxicology | fisheries | global change | mercury contamination

Human activity has increased the global mercury (Hg) pool by a factor of three to five since preindustrial times (1). Currently, anthropogenic Hg composes approximately two-thirds of the total Hg cycling worldwide (2). Hg deposition to terrestrial and aquatic ecosystems is predominantly in the form of inorganic Hg (IHg). However, biotic reactions (3) can convert IHg into methylmercury (MeHg)—a persistent toxic form that bioaccumulates through food webs. The extent to which historical (e.g., pre-1940) and current (e.g., post-1990) anthropogenic Hg emissions have affected biota remains to be fully elucidated (4–6). Both the Environmental Protection Agency (7) and the National Institutes of Health (8) have highlighted an alarming lack of data on the bioaccumulation of MeHg in aquatic food webs and its impacts on avian wildlife, especially piscivorous species.

Extensive museum collections comprise invaluable resources to examine temporal trends in avian MeHg exposure (used synonymously with bioavailable Hg exposure). Dietary MeHg accumulates in body tissues (9). During feather growth, tissue MeHg associates with disulfide bridges of keratin (10) to form strong, stable bonds that withstand rigorous physical treatments over time (11). Exposure of avifauna to bioavailable Hg may thereby be studied reliably through feathers from dated, preserved skins. Virtually all of the diet-derived Hg incorporated into feathers is in the form of MeHg (12). Consequently, total Hg is often measured to estimate MeHg as a more cost-effective alternative to direct MeHg quantification. However, museum curators traditionally applied preservatives that contained IHg (13). This contamination along with its scarce documentation has rendered total Hg measurement (IHg + MeHg) questionable for studying bioavailable Hg exposure in historical museum specimens.

To the best of our knowledge, only four studies have directly quantified MeHg in museum specimens of piscivorous birds across century-long time periods. Increases were observed in 9 of 10 Atlantic species (14, 15), 2 of 2 German North Sea species (16), and 0 of 6 sub-Arctic species (17). Nonetheless, no prior research has studied comparably extensive temporal trends in MeHg levels for a species from the Pacific, which harbors one-half of the world's seabird species and more threatened seabird species per unit of land area than any other ocean (18). Moreover, previous historically broad assessments of MeHg in birds have measured neither IHg nor stable isotopes to analyze concurrently factors that may have influenced exposure of the specimens to Hg over time. The ratio of stable isotopes of nitrogen ($\delta^{15}N$) is thought to be an indicator of trophic level, whereas the ratio of carbon ($\delta^{13}C$) reflects food sources (19). Both trophic level and diet mediate MeHg exposure and bioaccumulation (20).

To clarify the trends in MeHg and IHg exposure in a pelagic piscivore from the Pacific and to identify concomitant changes in avian ecology, we used museum skins of the black-footed albatross (*Phoebastria nigripes*) collected between 1880 and 2002. Hg contamination in the Pacific Ocean warrants our attention because, although most continents have reduced emissions over the past two decades, Asian emissions during 1990–2005 nearly doubled (21, 22). Asia now continues to contribute 67% of global anthropogenic Hg emissions, with over one-half of Asian emissions attributed to sources in China. The black-footed albatross, a wide-ranging, keystone predator, serves as an ideal sentinel species for determining the effect of both global increases in Hg throughout the previous century and regional increases during the most recent decades on bioaccumulation and risk among avian wildlife. Of 12 different Pacific seabird species, black-footed al-

Author contributions: A.E.V., M.S.B., J.P.S., and S.V.E. designed research; A.E.V. performed research; M.S.B. and J.P.S. contributed new reagents/analytic tools; A.E.V. analyzed data; and A.E.V., M.S.B., J.P.S., and S.V.E. wrote the paper.

The authors declare no conflict of interest.

This article is a PNAS Direct Submission. J.N. is a guest editor invited by the Editorial Board.

Freely available online through the PNAS open access option.

[1]To whom correspondence should be addressed. E-mail: sedwards@fas.harvard.edu.

This article contains supporting information online at www.pnas.org/lookup/suppl/doi:10.1073/pnas.1013865108/-/DCSupplemental.

batrosses exhibit among the highest feather concentrations of total Hg (23). We quantified total Hg in black-footed albatrosses from two major museum collections, focusing the full analysis (MeHg, IHg, and stable isotopes of nitrogen and carbon) on an available subset (46%) of samples that spanned the entire period of investigation. As controls to identify potential contamination from the use of museum preservatives over a similar temporal span, we also quantified IHg in two terrestrial avian species, russet-crowned motmots (*Momotus mexicanus*) and Altamira orioles (*Icterus gularis*), whose exposure to bioavailable MeHg in the wild is minimal (24, 25). Our comparison of MeHg and IHg trends among all species as well as with records of anthropogenic Hg emissions and curatorial practices shows unambiguous increases in MeHg bioaccumulation in marine biota and decreases in external Hg contamination of museum collections over time.

Results

Methylmercury Exposure in Black-Footed Albatrosses over Time. Concentrations of total Hg in the breast feathers of black-footed albatross museum specimens (n = 54) (Dataset S1) did not exhibit a temporal trend (Fig. 1). However, mean MeHg levels were significantly higher in post-1940 (35,750 ng·g^{-1}, n = 16) specimens relative to pre-1940 (22,330 ng·g^{-1}, n = 9) specimens (t = 1.754, df = 22, P = 0.047) as well as in post-1990 (42,130 ng·g^{-1}, n = 10) specimens relative to pre-1990 (23,450 ng·g^{-1}, n = 15) specimens (t = −1.824, df = 11, P = 0.048) (Figs. 1 and 2). The proportion of post-1940 specimens (6 of 16) with MeHg levels above estimated adverse thresholds, ∼5,000–40,000 ng·g^{-1} (26, 27), was significantly greater (P = 0.045; one-tailed Fisher's exact test) than that of pre-1940 specimens (0 of 9). Similarly, the proportion of post-1990 (5 of 10) specimens with MeHg levels above 40,000 ng·g^{-1} was significantly higher (P = 0.023; one-tailed Fisher's exact test) relative to pre-1990 specimens (1 of 15).

To help explain the observed trend in MeHg bioaccumulation over time, we obtained additional data from two stable isotopes, δ^{15}N and δ^{13}C. δ^{15}N values did not change substantially over the 120-y period (mean = 17.9‰, adjusted R^2 = −0.050, P = 0.924) (Fig. S1*A*). In contrast, δ^{13}C values declined significantly (adjusted R^2 = 0.228, P = 0.014) (Fig. S1*B*). We sought to identify those factors among a suite of a priori predictors [year, trophic level (δ^{15}N), carbon source (δ^{13}C), and body size (tarsus length)] most associated with temporal variation in the albatross MeHg levels. A multiple linear regression including all predictors significantly explained MeHg variation among samples. However, the model incorporating year (β = 0.003, P = 0.074), δ^{15}N (β = 0.142, P = 0.006), and tarsus length (β = 0.006, P = 0.723) explained the most variance in the MeHg dataset (Table 1 and *SI Results, Multiple Regression for MeHg Concentration in Black-Footed Albatross*), with δ^{15}N having the strongest effect (P = 0.007, w_i = 0.80) followed by year (P = 0.049, w_i = 0.13) (Fig. 1) and tarsus length (P = 0.083, w_i = 0.08). Although mean δ^{15}N or trophic position of the albatrosses did not change appreciably over time, variation in trophic position among samples of any given year explained a significant portion of the variability in feather MeHg levels. Carbon source did not strongly correlate with MeHg concentration.

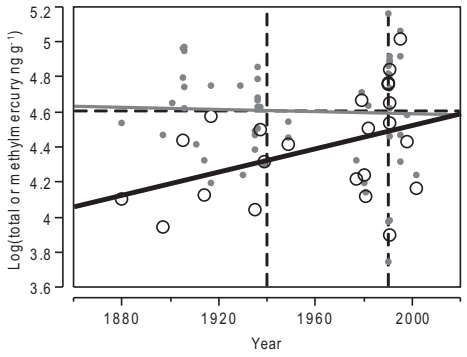

Fig. 1. Temporal trends in total mercury and methylmercury concentrations in the breast feathers of black-footed albatross museum specimens spanning 1880–2002. Gray points and solid line show log(total mercury ng·g^{-1}) = 5.198–0.0003 × year. Adjusted R^2 = 0.018, P = 0.775, and n = 53, excluding one outlier. Black open circles and solid line show log(methylmercury ng·g^{-1}) = −4.671 + 0.003 × year + 0.006 × tarsus + 0.143 × δ^{15}N. Adjusted R^2 = 0.385, P = 0.006, and n = 23 of the above 53 samples, excluding two outliers (one each for tarsus length and δ^{15}N) according to the best-fit model from a corresponding multiple regression analysis. Dotted horizontal line indicates adverse effect threshold of log (40,000 ng·g^{-1}). Dotted vertical lines indicate the years 1940 and 1990.

Inorganic Mercury Contamination of Avian Museum Specimens over Time. Despite an increase in MeHg exposure over time among black-footed albatrosses, there was a strong and significant decrease in IHg concentration (Fig. 3). The observed IHg decline was recapitulated among our two control species, russet-crowned motmots and Altamira orioles (Fig. 3 and Fig. S2*B*), chosen because we expected their life history traits to incur negligible exposure to MeHg. Confirming expectations, we observed low MeHg and nontrending concentrations in the control specimens throughout the 120-y time span (*SI Results, MeHg in Russet-Crowned Motmots and Altamira Orioles* and Fig. S3), indicating that the Hg found in these species was mainly caused by curatorial contamination. There was no significant difference in means of IHg concentrations between the motmots and orioles when paired by decade (t = 6.145, df = 6, P = 0.534). Furthermore, for the two control species as well as for black-footed albatrosses, there was no effect of collection locality on observed decreases in IHg concentration over time.

Discussion

Methylmercury Bioaccumulation and Anthropogenic Mercury Output. This study characterizes both total Hg and MeHg exposure over a 120-y time span (1880–2002) for a species inhabiting the Pacific region and complements this dataset with stable isotopes analysis to assess the influence of ecological factors on observed MeHg trends. Strict quality control and replicate measurements for all four analytical procedures supported measurement accuracy and precision. Variation in the original feather mass destructively sampled from museum specimens of this endangered species restricted our analysis of all factors to a subset of specimens with sufficient material to develop our dataset. Nevertheless, we have detected a significantly increasing trend in MeHg, which may have important ecotoxicological implications for Pacific vertebrates.

The δ^{15}N data suggest that mean trophic level did not change over time, whereas a number of potentially correlated phenomena may underlie the temporal trend in δ^{13}C. Differing from our results for the pelagic black-footed albatross, temporal shifts in trophic level have been observed in at least one Pacific albeit coastal seabird species (*SI Discussion, Temporal Trend in δ^{15}N*). Increased anthropogenic output of fossil fuel-derived carbon dioxide (CO_2), which is depleted in ^{13}C relative to the atmosphere, may have resulted in the decrease in δ^{13}C over time known as the Suess effect (28). Consistent declines in marine primary productivity can also produce signatures of reduced δ^{13}C values (29). Alternatively, gradual shifts in foraging localities (30) or consumption of benthic vs. pelagic prey (31) over time may likewise result in consistent changes in δ^{13}C values. We rule out the first three possibilities based on the (*i*) application of the correction by Schelske and Hodell (32) for the Suess effect, (*ii*) expected effects of the Pacific Decadal Oscillation on marine primary productivity (33), and (*iii*) historical observations of the foraging range for the species (34), respectively. Changes in diet remain potential drivers

Table 1. Model selection table from multiple linear regression analysis using year, $\delta^{13}C$ (corrected for the Suess effect), $\delta^{15}N$, and tarsus length (cm) to predict log(methylmercury concentration ng·g^{-1}) in black-footed albatross breast feathers

Model	n*	$K^{\dagger}$	$R^{2\ddagger}$	$P^{\S}$	RSS¶	AIC$^{\|}$	AIC$_c$**	ΔAIC$_c$	$w_i^{\dagger\dagger}$
1. Year + $\delta^{15}N$ + tarsus length	23	3	0.385	0.006	1.057	4.43	5.69	0.00	0.58
2. Year + δ15N	24	2	0.291	0.010	1.309	6.30	6.87	1.18	0.32
3. Year + corrected $\delta^{13}C$ + $\delta^{15}N$ + tarsus length	22	4	0.321	0.030	1.020	6.87	9.22	3.53	0.10

*Sample size.
†Number of parameters.
‡Adjusted R^2.
§P value.
¶Residual sum of squares.
‖Akaike's information criterion.
**Akaike's information criterion corrected for small sample size.
††Akaike weight.

of changes in black-footed albatross $\delta^{13}C$ over time (further discussion in *SI Discussion, Temporal Trend in $\delta^{13}C$*), although long-term, species-specific temporal data on prey items are unavailable for the direct assessment of alterations in diet composition.

Our models explored the relative influence of food source ($\delta^{13}C$), trophic position ($\delta^{15}N$), body size (tarsus length), and year on MeHg exposure in black-footed albatrosses. Despite the observed $\delta^{13}C$ temporal trend, the models revealed that $\delta^{13}C$ was a nonsignificant factor. $\delta^{15}N$ strongly explained variation in black-footed albatross feather MeHg levels at any given point in time. Additionally, after controlling for the influence of $\delta^{15}N$ variation among samples on MeHg feather levels, year remained as a significant explanatory factor for MeHg variation. Identification of the underlying changes in historical and current MeHg sources is, consequently, of concern. High resolution, temporal data for historical Hg emissions on both the global and regional scales are limited, but preindustrial depositions have been estimated to be 500 tons/y (1). In the 1940s, when global demand during World War II played a prominent role, global Hg release increased substantially from mineral mining and fossil fuel combustion, and high levels of Hg production and consumption were sustained until the 1990s (22, 35). Total annual anthropogenic Hg emissions rose from low preindustrial values to 1,930 tons in 2005 (22). Moreover, since the 1990s, annual Hg emissions from Asia have increased from ~700 tons in 1990 to 1,290 tons in 2005 (21, 22, 36). Asia's contribution has comprised an increasingly greater proportion of global totals, with China as the largest emitter of Hg worldwide at 635 tons in 2005.

There has been considerable debate as to whether anthropogenic sources can or have affected wide-ranging biota within marine systems. It was predicted in 1971 that, if evenly mixed across the world's oceans, the total anthropogenic increase in Hg flux would result in a doubling of Hg concentrations in the upper 100 m of the oceans, and this increase could amplify through the food web to upper trophic levels (37). However, three studies to date have examined temporal trends in total Hg levels within tissues of pelagic and benthopelagic marine fish species, and they have failed to observe increases (4, 5, 38). Higher trophic levels among black-footed albatrosses and other seabirds (14–16) relative to fish may explain the positive trend in MeHg exposure over time in the former, despite the lack of trends in the latter.

The scarcity of explicit, century-wide, temporal data on anthropogenic Hg emissions prevented a more rigorous correlational analysis with the albatross MeHg data, and our attempts to correlate our data with proxies for atmospheric Hg deposition over the last 270 y yielded nonsignificant results (*SI Discussion, Correlation Between Black-Footed Albatross MeHg and Upper Fremont Glacier Dataset*). Reasons that may explain the absence of a tight correlation between the datasets include error in ice-core concentrations as accurate proxies of global emission levels, lag times in the conversion of emissions into bioavailable forms,

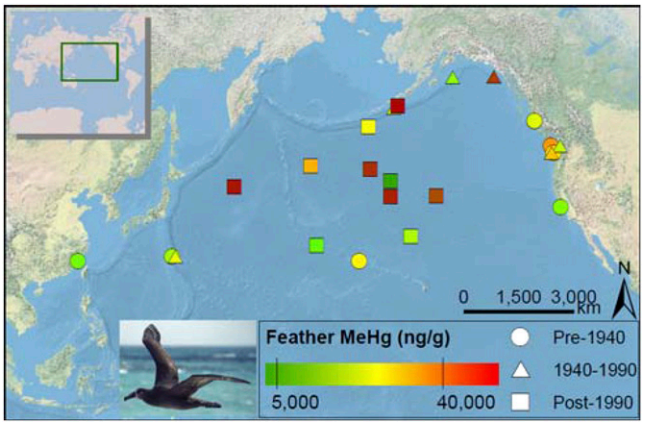

Fig. 2. Collection localities and methylmercury concentrations measured in the breast feathers of black-footed albatross museum specimens from the Harvard University Museum of Comparative Zoology (n = 8) and University of Washington Burke Museum of Natural History and Culture (n = 17). Lowest (5,000 ng·g^{-1}) and highest (40,000 ng·g^{-1}) adverse effect thresholds for birds are indicated on the color ramp. Albatross photo by S.V.E.

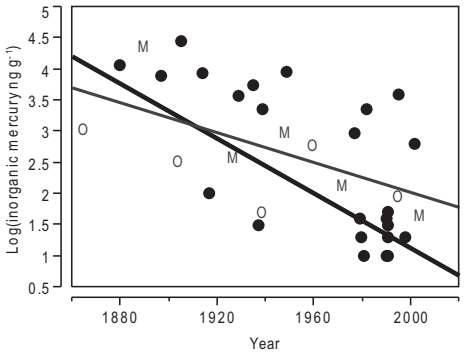

Fig. 3. Temporal trends in inorganic mercury concentrations in the breast feathers of black-footed albatross (BFAL) museum specimens spanning 1880–2002 (n = 25) and russet-crowned motmot (M; n = 5) and Altamira oriole (O; n = 5) museum specimens spanning 1865–2004. Black line shows BFAL: log(inorganic mercury ng·g^{-1}) = 45.127 − 0.022 × year, adjusted R^2 = 0.431, and P = 0.0002. Gray line shows M and O: log(inorganic mercury ng·g^{-1}) = 26.023 − 0.012 × year, adjusted R^2 = 0.391, and P = 0.032.

and nonlinear uptake of MeHg in top trophic-level predators over time. Nevertheless, Hg assessments of numerous abiotic matrices within the Pacific region as well as both abiotic and biotic matrices from various worldwide localities have consistently revealed increases in Hg deposition and exposure over historical and recent time (Table S1). Our study contributes to these growing lines of evidence for the impact of anthropogenic Hg emissions on oceanic systems. Black-footed albatross MeHg exposure seems to be in accordance with the post-1940 global anthropogenic Hg flux, as found in other Atlantic seabird species (14), and also with the post-1990 spike in Asian Hg emissions for the Pacific region. Despite the importance of emissions data, direct MeHg measurements in historical organisms are ultimately needed to assess species risk.

Current Status of the Black-Footed Albatross. Species-specific sublethal effects thresholds for white-tailed eagles and common loons suggest that anywhere from 5,000 to 40,000 $ng{\cdot}g^{-1}$ in feathers may result in fitness declines (26, 27). If these determinations are applicable to black-footed albatrosses, using the conservative 40,000 $ng{\cdot}g^{-1}$ upper limit of the sublethal threshold range, we estimate that a proportion of albatrosses may have begun experiencing deleterious Hg effects in the early 1980s (Fig. 1). Over one-half of our most recent, post-1990 samples contained MeHg levels above 40,000 $ng{\cdot}g^{-1}$. Chronic MeHg exposure can potentially undermine population growth within the species. Black-footed albatross reproductive biology involves delayed maturation, single-egg clutches, and biannual breeding attempts—all of which predispose the species to low reproductive success (39). Within the pelagic range of the black-footed albatross (40, 41), deposition and lateral transport along ocean currents have, respectively, resulted in detectable Hg enrichment of western coastal waters and eastern intermediate waters of the North Pacific (42). Rapid, basin-wide rises in Hg levels are predicted if current Asian emissions are sustained. Given the existing elevated MeHg loads among black-footed albatrosses and the vulnerability of these birds to several other toxic marine contaminants (43), concerns are raised for more serious future population impacts.

Implications for Using Museum Specimens in Mercury Studies. Over 5 million bird specimens are housed in museum collections throughout North America, offering researchers extraordinary potential to pursue diverse questions regarding the trophic transfer and bioaccumulation of MeHg in numerous species. However, among many factors, sampling designs must carefully consider the effects of collection locality, breeding season, sex, museum origin, and external Hg contamination of the specimens. The former four factors did not seem to significantly influence observed MeHg concentrations among black-footed albatrosses in this study (*SI Discussion, Influence of Black-Footed Albatross Collection Locality, Breeding Season, Sex, and Museum Origin on MeHg and Stable Isotopes*). Regarding external contamination, documentation of Hg-containing preservative use is lacking for most museums. However, the observed decrease in IHg over time for all three study species occurs after the time frame (late 1800s through 1930s) of widespread mercuric chloride ($HgCl_2$) use in the Smithsonian Institution National Museum of Natural History (NMNH) (44) and thus, may reflect a similar history of preservative application among several museum collections in the United States.

Our results indicate that, when using museum specimens, MeHg quantification is necessary to accurately assess bioavailable Hg exposure over historical time. Preparation and storage conditions are unlikely to alter the MeHg content of specimens given the bond strength of diet-derived MeHg to keratin (10, 11) and the general lack of external sources of MeHg contamination (*SI Discussion, Abiotic Methylation of IHg in Museum Specimens*) (45). Although more cost-effective, measurement of total Hg can obscure temporal signal of MeHg exposure (Fig. 1) because IHg may comprise as much as one-half of the total Hg in the oldest specimens. However, IHg in post-1980 specimens comprises 5% or less of total Hg, which may render total Hg values suitable for studies based on recent museum collections.

Conclusions

In addition to illustrating the value of museum specimens for temporal assessments of environmental contaminants, our dataset characterizes multiple environmental signatures (total Hg, MeHg, and IHg as well as carbon and nitrogen stable isotopes) across a 120-y period in a flagship, pelagic species, the black-footed albatross. Together, our data suggest that, if prey shifts occurred over the period of our study, historical and current prey comprised similar trophic levels. Nonetheless, increased exposure of prey to MeHg may explain the observed increases in albatross feather MeHg to levels above estimated, adverse thresholds over time, which we found to be consistent with past global and contemporary regional anthropogenic Hg emissions. Additional studies on Pacific biota from different trophic positions and across multiple spatiotemporal scales are warranted to elucidate the ecotoxicological implications of continued anthropogenic Hg output to the environment.

Methods

Museum Collections and Sampling. We obtained breast contour feathers from black-footed albatross preserved skin specimens (Dataset S1 and Fig. S2*A*) in the Harvard University Museum of Comparative Zoology (MCZ; $n = 23$ of 26 total available skins from 1880 to 1949) and the University of Washington Burke Museum of Natural History and Culture (UWBM; $n = 31$ of 95 total available skins from 1917 to 2002). We sampled all accessible MCZ specimens and then randomly sampled UWBM specimens among stratified decades to maximize temporal spread. Body contour feathers have been shown to be most representative of total body MeHg burden (9). We found no preliminary difference in mean total Hg between paired feathers sampled from the left and right sides of the breast ($t = -1.182$, $P = 0.303$, $n = 5$). Therefore, we sampled a single central breast contour feather from all remaining individuals. Because black-footed albatrosses range widely throughout the Pacific Ocean while foraging within a lifetime (39, 46, 47), we did not expect differences in collection locality to confound signals of temporal variation in bioavailable Hg exposure. We similarly sampled central breast feathers for Hg analysis from russet-crowned motmots and Altamira orioles. These species are nonmigratory, terrestrial, and nonpiscivorous, and they are distributed within relatively poorly industrialized countries (Fig. S2*B*).

Total Hg and MeHg Measurements. Feathers were washed, dried, and homogenized (*SI Methods, Sample Preparation*). We measured total Hg in 0.0010 g homogenate per sample using thermal decomposition, amalgamation, and atomic absorption spectrophotometry [Environmental Protection Agency (EPA) method 7473; US EPA] under an automated analyzer (DMA-80 Mercury Analyzer; Milestone Inc.). Certified reference materials (marine sediment MESS-3 and dogfish liver DOLT-3; National Research Council Canada, Ottawa) and procedural blanks were analyzed after every 10 samples to ensure instrument accuracy and establish detection limits. To estimate precision, we measured each black-footed albatross feather sample in triplicate (mean coefficient of variation = 21.43%). Quality assurance and quality control results are presented in *SI Methods* (*SI Methods, Total Hg Measurements*).

To quantify the IHg and MeHg components of total Hg in the black-footed albatross breast feathers, we analyzed (at the Dartmouth College Trace Metals Analytical Laboratory, Hanover, NH) a subset of the MCZ ($n = 8$, 1880–1949) and UWBM ($n = 17$, 1917–2002) samples representative of maximal temporal spread. All russet-crowned motmot and Altamira oriole samples were analyzed with the same procedure. Samples were extracted in KOH/MeOH (25% mass/volume). After addition of enriched methylmercury ($Me^{201}Hg$), samples were sonicated and shaken overnight. Subsamples of each extract were assessed by purge and trap thermal desorption GC inductively coupled plasma MS (GC-ICP-MS): Hg species were ethylated, trapped in Tenax traps (Brooks Rand), separated by thermal desorption packed column GC, and quantified by isotope dilution ICP-MS (*SI Methods, MeHg Measurements*).

Stable Isotope Measurements. We also analyzed the same subset of MCZ and UWBM black-footed albatross feather samples that underwent MeHg analyses for carbon (C) and nitrogen (N) stable isotope ratios at the Stable Isotope Laboratory at Boston University (Boston, MA). Organic C and N were converted into CO_2 and N_2 gas and were quantified using an Isoprime isotope mass spectrometer (GV Instruments) and Eurovector elemental analyzer (Eurovector). $^{13}C/^{12}C$ and $^{15}N/^{14}N$ ratios were assessed in both study samples and standards, where Vienna Peedee Belemnite and atmospheric nitrogen were used for carbon and nitrogen standards, respectively (*SI Methods, Stable Isotope Measurements*). Results are shown as deviations from standards expressed as $\delta^{13}C$ and $\delta^{15}N$ using the formula $\delta X = (R_{smpl}/R_{stnd} - 1) \times 10^3$, where X is ^{13}C or ^{15}N and R is $^{13}C/^{12}C$ or $^{15}N/^{14}N$.

Statistical Analyses. We averaged total Hg replicate values to represent each sample (*SI Methods, Statistical Analysis, Total Hg replicate measurements*). We compared the proportion of albatrosses with MeHg concentrations above the highest sublethal threshold established for birds (40,000 ng·g^{-1}) between pre- and post-1940 samples as well as pre- and post-1990 samples using Fisher's exact test. We chose the years 1940 and 1990 to reflect historical global increases in Hg mobilization because of World War II and recent regional increases of Hg emissions in the Asian Pacific. We also used Student's t tests assuming unequal variances to compare mean MeHg concentrations between (*i*) pre- and post-1940 samples, (*ii*) pre- and post-1990 samples, (*iii*) albatrosses (n = 22) and motmots (n = 5), and (*iv*) albatrosses (n = 22) and orioles (n = 5). We performed the latter two tests on log-transformed datasets to meet normality.

For regression analyses, we log-transformed all Hg concentrations to meet normality and excluded outliers from each dataset (*SI Methods, Statistical Analysis, Outliers*). We used simple linear regression to evaluate the relationship between (*i*) IHg and year for the combined motmot and oriole dataset (*SI Methods, Statistical Analysis, Motmot and oriole dataset*), (*ii*) total Hg and year for all albatross samples (n = 54), (*iii*) IHg and year for the subset of albatross samples that underwent speciation analysis (n = 25), and (*iv*) IHg and year as well as (*v*) MeHg and year for motmot (n = 5) and oriole (n = 5) samples. We used multiple linear regression to analyze the relationship between year (n = 25), tarsus length (n = 24, excluding one outlier) as a proxy for body size (48), trophic position ($\delta^{15}N$; n = 24, excluding one outlier), carbon source ($\delta^{13}C$; n = 24, excluding one outlier), and MeHg concentration (n = 25) for the albatross subset (*SI Methods, Statistical Analysis, Model determination*). The correction by Schelske and Hodell (32) for the Suess effect, the increase in anthropogenic fossil fuel-derived CO_2 in the atmosphere over historical time, was applied to the $\delta^{13}C$ data before it was used in the regression analysis (*SI Methods, Statistical Analysis, $\delta^{13}C$ correction*). We used Akaike's information criterion corrected for small sample sizes (AIC_c) and Akaike's weights (w_i) to select the best model (*SI Methods, Statistical Analysis, Model evaluation*). The presented bivariate plot of MeHg over time was generated from the parameters of the best model.

Finally, we assessed the strength of correlation between MeHg levels in black-footed albatrosses and total Hg levels as well as total Hg deposition rates in the Upper Fremont Glacier using linear regression for the largest overlapping historical period, 1880–1995, between the datasets. We included all albatrosses from the best multiple regression model in this analysis (n = 23). We paired MeHg levels with measured total Hg levels or total Hg deposition rates in the glacier core layer that corresponded closest to the collection year of the albatross specimen.

All analyses were completed in R 2.7.2 (The R Foundation for Statistical Computing), and all graphs were developed in JMP 9.0 (SAS Institute). Tests used to determine whether the data met regression assumptions and an evaluation of sampling methods have been included as supporting information (*SI Methods, Statistical Analysis, Tests for regression assumptions*).

ACKNOWLEDGMENTS. We thank J. Trimble of the Harvard Museum of Comparative Zoology, R. C. Faucett of the University of Washington Burke Museum, R. Corado of the Western Foundation of Vertebrate Zoology, P. Sweet of the American Museum of Natural History, R. C. K. Bowie and C. Cicero of the University of California Berkeley Museum of Vertebrate Zoology, and J. Klicka of the University of Nevada Las Vegas Marjorie Barrick Museum for sampling and loan assistance. We thank R. Michener (Boston University, Stable Isotope Laboratory, Boston, MA) for stable isotopes analyses, B. Jackson (Dartmouth College, Trace Metals Laboratory, Hanover, NH) for Hg speciation analyses, B. Rosner for statistical advice, P. F. Schuster for Upper Fremont Glacier data, J. Trimble for helpful discussion, and A. Amirbahman, G. Graves, G. Nevitt, and several anonymous reviewers for thoughtful comments on earlier versions of the manuscript. Financial support was provided by a Museum of Comparative Zoology Grant-in-Aid of Undergraduate Research (to A.E.V.), the Harvard Program for Research in Science and Engineering (PRISE) program, a grant from the Harvard University Museum of Comparative Zoology (to M.S.B.), and the Harvard College Research Program.

1. Selin NE (2009) Global biogeochemical cycling of mercury: A review. *Annu Rev Env Resour* 34:43–63.
2. Lindberg S, et al. (2007) A synthesis of progress and uncertainties in attributing the sources of mercury in deposition. *Ambio* 36:19–33.
3. Hammerschmidt CR, Fitzgerald WF (2004) Geochemical controls on the production and distribution of methylmercury in near-shore marine sediments. *Environ Sci Technol* 38:1487–1495.
4. Miller GE, et al. (1972) Mercury concentrations in museum specimens of tuna and swordfish. *Science* 175:1121–1122.
5. Kraepiel AML, Keller K, Chin HB, Malcolm EG, Morel FM (2003) Sources and variations of mercury in tuna. *Environ Sci Technol* 37:5551–5558.
6. Chen C, et al. (2008) Methylmercury in marine ecosystems: Spatial patterns and processes of production, bioaccumulation, and biomagnification. *Ecohealth* 5:399–408.
7. United States Environmental Protection Agency (2000) *Mercury Research Strategy EPA/600/R-00/073* (United States Environmental Protection Agency, Washington DC).
8. Chen CY, et al. (2008) Meeting report: Methylmercury in marine ecosystems—from sources to seafood consumers. *Environ Health Perspect* 116:1706–1712.
9. Furness RW, Muirhead SJ, Woodburn M (1986) Using bird feathers to measure mercury in the environment: Relationships between mercury content and moult. *Mar Pollut Bull* 17:27–30.
10. Crewther WG, Fraser RD, Lennox FG, Lindley H (1965) The chemistry of keratins. *Adv Protein Chem* 20:191–346.
11. Appelquist H, Asbirk S, Drabæk I (1984) Mercury monitoring: Mercury stability in bird feathers. *Mar Pollut Bull* 15:22–24.
12. Thompson DR, Furness RW (1989) Comparison of the levels of total and organic mercury in seabird feathers. *Mar Pollut Bull* 20:577–579.
13. Palmer PT (2001) A review of analytical methods for the determination of mercury, arsenic, and pesticide residues on museum objects. *Collection Forum* 16:25–41.
14. Thompson DR, Furness RW, Walsh PM (1992) Historical changes in mercury concentrations in the marine ecosystem of the north and north-east Atlantic ocean as indicated by seabird feathers. *J Appl Ecol* 29:79–84.
15. Monteiro LR, Furness RW (1997) Accelerated increase in mercury contamination in north Atlantic mesopelagic food chains as indicated by time series of seabird feathers. *Environ Toxicol Chem* 16:2489–2493.
16. Thompson DR, Becker PH, Furness RW (1993) Long-term changes in mercury concentrations in herring gulls Larus argentatus and common terns *Sterna hirundo* from the German North Sea coast. *J Appl Ecol* 30:316–320.
17. Thompson DR, Furness RW, Lewis SA (1993) Temporal and spatial variation in mercury concentrations in some albatrosses and petrels from the sub-Antarctic. *Polar Biol* 13: 239–244.
18. BirdLife International (2009) *Pacific Programme 2009–2012* (BirdLife International, Australia).
19. Michener RH, Lajtha K (2007) *Stable Isotopes in Ecology and Environmental Science* (Wiley-Blackwell, New York).
20. Boudou A, Ribeyre F (1997) in *Mercury and Its Effects on Environment and Biology*, eds Sigel A, Sigel H (Marcel Dekker, Inc., New York), pp 289–319.
21. AMAP/UNEP (2008) Technical background report to the global atmospheric mercury assessment. Arctic Monitoring and Assessment Programme/UNEP Chemicals Branch 159 pp.
22. Pacyna EG, et al. (2010) Global emission of mercury to the atmosphere from anthropogenic sources in 2005 and projections to 2020. *Atmos Environ* 44:2487–2499.
23. Burger J, Gochfeld M (2000) Metal levels in feathers of 12 species of seabirds from midway atoll in the northern Pacific Ocean. *Sci Total Environ* 257:37–52.
24. Forcey JM (2002) Notes on the birds of central oaxaca, part II: Columbidae to vireonidae. *Huitzil* 3:14–27.
25. Brush T, Pleasants BY (2005) *Altamira Oriole (icterus gularis). Birds of North America Online < Bna.Birds.Cornell.edu/BNA/account/Altamira_Oriole* (Cornell Laboratory of Ornithology, Ithaca, NY).
26. Eisler R (1987) Mercury hazards to fish, wildlife, and invertebrates: A synoptic review. *U.S. Fish and Wildlife Service: Biological Report 85: 1.10* (Patuxent Wildlife Research Center, Laurel, MD).
27. Evers DC, et al. (2008) Adverse effects from environmental mercury loads on breeding common loons. *Ecotoxicology* 17:69–81.
28. Suess HE (1955) Radiocarbon concentration in modern wood. *Science* 122:415–417.
29. Schell DM, Barnett BA, Vinette KA (1998) Carbon and nitrogen isotope ratios in zooplankton of the Bering, Chukchi and Beaufort seas. *Mar Ecol Prog Ser* 162: 11–23.
30. Cherel Y, Hobson KA (2007) Geographical variation in carbon stable isotope signatures of marine predators: A tool to investigate their foraging areas in the Southern Ocean. *Mar Ecol Prog Ser* 329:281–287.
31. Bearhop S, Waldron S, Votier SC, Furness RW (2002) Factors that influence assimilation rates and fractionation of nitrogen and carbon stable isotopes in avian blood and feathers. *Physiol Biochem Zool* 75:451–458.

32. Schelske CL, Hodell DA (1995) Using carbon stable isotopes of bulk sedimentary organic matter to reconstruct the history of nutrient loading and eutrophication in Lake Erie. *Limnol Oceanogr* 40:918–929.
33. Mantua NJ, Hare SR (2002) The Pacific decadal oscillation. *J Oceanogr* 58:35–44.
34. Lewison RL, Crowder LB (2003) Estimating fishery bycatch and effects on a vulnerable seabird population. *Ecol Appl* 13:743–753.
35. Swain EB, et al. (2007) Socioeconomic consequences of mercury use and pollution. *Ambio* 36:45–61.
36. Pacyna EG, Pacyna JM, Steenhuisen F, Wilson S (2006) Global anthropogenic mercury emission inventory for 2000. *Atmos Environ* 40:4048–4063.
37. Weiss HV, Koide M, Goldberg ED (1971) Mercury in a greenland ice sheet: Evidence of recent input by man. *Science* 174:692–694.
38. Barber RT, Vijayakumar A, Cross FA (1972) Mercury concentrations in recent and ninety-year-old benthopelagic fish. *Science* 178:636–639.
39. Rice DW, Kenyon KW (1962) Breeding distribution, history and populations of North Pacific albatrosses. *Auk* 79:365–386.
40. Kuroda N (1955) Observations on pelagic birds of the northwest Pacific. *Condor* 57:290–300.
41. Sanger GA (1974) in *Pelagic Studies of Seabirds in the Central and Eastern Pacific Ocean*, ed King WB (Smithsonian Institution Press), pp 96–126.
42. Sunderland EM, Krabbenhoft DP, Moreau JW, Strode SA, Landing WM (2009) Mercury sources, distribution, and bioavailability in the North Pacific Ocean: Insights from data and models. *Global Biogeochem Cycles* 23:1–14.
43. Finkelstein M, et al. (2006) Albatross species demonstrate regional differences in North Pacific marine contamination. *Ecol Appl* 16:678–686.
44. Goldberg L (1996) A history of pest control measures in the anthropology collections, National Museum of Natural History, Smithsonian Institution. *J Am Inst Conserv* 35: 23–43.
45. Furness RW, Camphuysen KCJ (1997) Seabirds as monitors of the marine environment. *ICES J Mar Sci* 54:726–737.
46. Hyrenbach KD, Fernández P, Anderson DJ (2002) Oceanographic habitats of two sympatric North Pacific albatrosses during the breeding season. *Mar Ecol Prog Ser* 233:283–301.
47. Kawakami K, et al. (2006) The foraging ranges of black-footed albatross diomedea nigripes breeding in the Bonin Islands, southern Japan, as determined by GPS tracking. *Ornitholog Sci* 5:187–191.
48. Senar JC, Pascual J (1997) Keel and tarsus length may provide a good predictor of avian body size. *Ardea* 85:269–274.